

Spatial variations of sea surface pCO₂ in the tropical Western Pacific near Guam

KyungJae Lee

University of Washington

School of Oceanography, Box 357940

Seattle, WA

98195-7940

kyungjae@uw.edu

3/14/2025

1 **Abstract**

2 The ocean sequesters carbon through solubility and biological pumps. It serves a critical
3 role in the sequestration of the atmosphere's carbon dioxide (CO₂). Understanding the extent of
4 its sequestration role is an essential tool in tackling climate change policies and protecting the
5 oceans. This study aims to understand the small-scale variabilities with increased levels of
6 anthropogenic CO₂ on the ocean's role as a sink of CO₂. This was done by collecting underway
7 temperature, salinity, sea surface partial pressure of CO₂ (pCO₂), atmospheric pCO₂ and
8 conditions continuously on the 2024-2025 University of Washington Oceanography Senior
9 Thesis Cruise between 4 °N-16 °N, 148 °E-149 °E. Small-scale spatial features of pCO₂
10 concentrations will be analyzed to find correlations with other parameters (temperature, salinity,
11 bathymetry) to find the driving process of the variations in pCO₂. Highest pCO₂ concentrations
12 were measured around the deepest sections of the Nam-2 Atoll and the furthest south. In
13 contrast, the lowest pCO₂ concentrations were measured around the Namonuito Guyot and
14 directly north of the 4 °N peaks, at 5.5 °N-6.2 °N. It was found that seamounts have a great
15 influence on pCO₂ concentrations. Since pCO₂ is relatively consistent in its vertical distribution,
16 local mixing due to currents accelerating against the seamount structures stirs higher
17 concentrations of pCO₂ into the mixed layer. This makes these areas with seamounts sources of
18 pCO₂. This will put the atmospheric pCO₂ concentrations into even higher saturation.

19 **Plain Language Summary**

20 Anthropogenic carbon dioxide (CO₂) emissions from fossil fuels have increased the
21 amount of CO₂ in our oceans as the global ocean absorbs the gases to reach equilibrium with the
22 atmosphere. The partial pressure of carbon dioxide (pCO₂) signifies the amount of CO₂ in the
23 ocean. As the oceans absorb more CO₂ through the solubility with water and photosynthesis,

24 they become increasingly saturated leading to regions becoming sources of CO₂. Therefore, it is
25 essential to collect data regionally to identify and help predict the current and future air-sea
26 fluxes as well as the main drivers of pCO₂ variability. This study aims to increase understanding
27 of the local variability in the sea surface of the western tropical Pacific from 4 °N-16 °N, 148
28 °E-149 °E. Data was collected from 29 December 2024-9 January 2025 on the R/V *Thomas G.*
29 *Thompson* using a continuous underway system that collected atmospheric pCO₂ data and
30 surface seawater to measure sea surface pCO₂ levels. A Thermosalinograph measured
31 temperature and salinity The main causes of anomalies in pCO₂ concentrations were identified as
32 biological processes, proximity to the equator, vertical local mixing, and changes in elevation of
33 the seafloor from underwater mountains (seamounts).

34 1. Introduction

35 Carbon dioxide (CO₂) has increased from about 277 parts per million dry air (ppm) to
36 424.60 ppm in 270 years in the atmosphere due to human activities (Friedlingstein et al., 2022;
37 Lan et al., 2023). The partial pressure of CO₂ (pCO₂) identifies the amount of carbon dioxide in
38 our oceans. Measurements taken in various parts of the world's oceans help to evaluate the
39 global and areal ocean net transport fluxes with the atmosphere, overall change in pCO₂,
40 biological effects on the seawater chemistry, and physical oceanographic processes such as
41 upwelling/downwelling, mixing, and current directions. The oceans are known to be a major sink
42 for CO₂, sequestering about 25% of anthropogenic CO₂ (Jiang et al., 2023). Understanding this
43 balance from a small-scale perspective is essential as different regions react in different ways in
44 response to climate change. The direction of net sea-air CO₂ transfer is determined by the
45 difference in atmospheric and sea surface CO₂, $\Delta p\text{CO}_2$, where if the $\Delta p\text{CO}_2$ is positive, CO₂ will
46 be absorbed by the ocean, but if $\Delta p\text{CO}_2$ is negative, then CO₂ will be released into the
47 atmosphere by the ocean due to oversaturated waters. This was analyzed throughout the region of
48 the cruise to find any area in which the ocean is a source of CO₂ and the outgassing of CO₂ into
49 the atmosphere occurs.

50 Several previous studies including Guo et al. (2024), Yasunaka et al. (2019), and Feely et
51 al. (2006) reported a negative correlation between sea surface pCO₂ and sea-surface
52 temperatures (SST). Typically, pCO₂ concentrations are found to be driven by SST in subtropical
53 gyres with weak vertical mixing and lower primary productivity (Guo et al. 2024). Primary
54 productivity assimilates CO₂ from the water and converts it into organic matter, causing lower
55 pCO₂ in areas of higher primary productivity. Colder SST aligned with higher pCO₂ levels since
56 colder waters can hold more gases, while high SST, such as the western subtropical Pacific, had

57 negative values of pCO₂. Primary productivity around Guam is low, SST is high, and thus would
58 be cause for lower pCO₂ concentrations that may be seen.

59 However, SST is increasing at a much more rapid rate than in the past. In the low-mid
60 latitude North Hemisphere, CO₂ uptake decreases during marine heatwaves by an average of
61 0.17 mol C (m² yr⁻¹) with this region and surrounding central equatorial Pacific experiencing the
62 greatest monthly CO₂ flux anomalies (Li 2024). Marine heatwaves are defined as periods of
63 constant abnormally warm ocean temperatures. As temperatures continue rising, it is essential to
64 have the data to contribute to global assessments. In the region of this study's data collection,
65 there was ~1 °Celsius (C) magnitude of marine heatwave (MHW) with a MHW probability of
66 30-60% beginning in December 2024 (Jacox et al. 2022).

67 Yasunaka et al. (2019) found that surface seawater pCO₂ ranged from 370–400 μatm
68 during February along 20 °N–5 °N at the 149 °E track when looking at the long-term mean from
69 1981-2015 (Fig. 1a). Like the Guo et al. (2024) study, pCO₂ was high when and where SST was

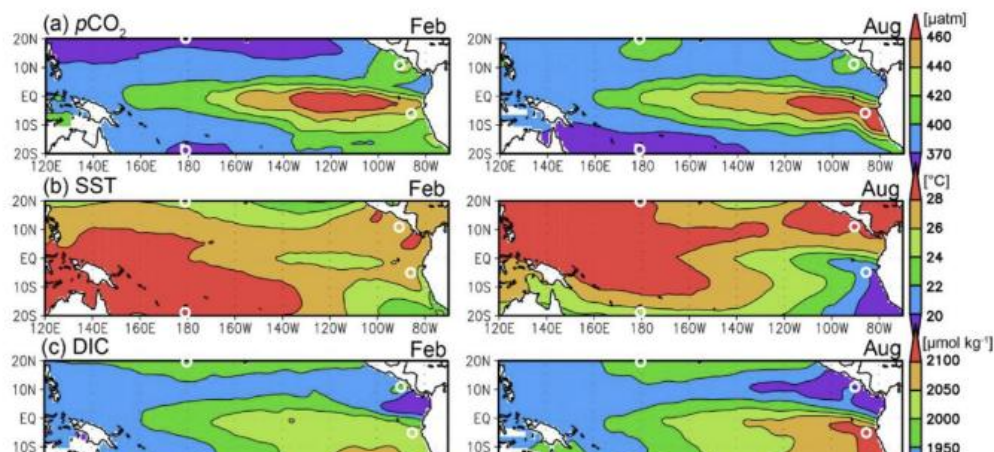


Figure 1. Long-term means from 1981-2015 with February on the left and August on the right (a-c). a) Seawater pCO₂ (μatm), b) SST (°C), c) DIC (μmol kg⁻¹). Area average of seawater pCO₂ was $1.8 \pm 0.07 \mu\text{mol yr}^{-1}$ while atmospheric pCO₂ average for the area was $1.7 \pm 0.01 \mu\text{mol yr}^{-1}$. (Figure from Yasunaka et al., 2019).

70 low. Based on these means, this study concluded that pCO₂ seasonal variation is driven by the
71 upwelling of colder, saltier subsurface carbon-rich water at the equator (Yasunaka et al. 2019).

72 Overall, pCO₂ concentrations will have increased since past data collections due to
73 continued anthropogenic emissions but the ocean is believed to remain a sink for atmospheric
74 CO₂. Spikes in pCO₂ concentrations are hypothesized to occur due to increased upwelling at
75 lower latitudes approaching the equator, while a decrease in pCO₂ will be due to higher
76 biological productivity near seamounts through the uptake of CO₂ through photosynthesis. If
77 there are no spikes or decreases in data, then none of these processes are pushing concentrations
78 in a positive or negative direction, and pCO₂ concentrations are in a steady state. This study aims
79 to increase understanding of the main drivers of pCO₂ concentrations, so that, as global
80 concentrations vary, more thorough predictions can be made with knowledge of how similar
81 types of regions will be affected by increasing atmospheric CO₂.

82 **2. Methods**

83 All the data used in this study are the results of direct pCO₂ measurements using the
84 Pacific Marine Environmental Laboratory Underway pCO₂ system during the cruise (Fig. 2). A
85 pump on this underway system continuously took in seawater from about five meters from the
86 bow of the ship and ran it through the SBE45 Thermosalinograph (TSG) TGT 0625 to measure
87 temperature and salinity. This seawater was run through the equilibrators for pCO₂ concentration
88 measurements. The pCO₂ system also has a non-dispersive infrared analyzer built by *LICOR*[®]
89 that measures pCO₂ in dry air, including atmospheric pCO₂, air pumped from the bow, and gas in
90 the equilibrators headspace. The analyzer measured four standards every two-and-a-half to three
91 hours, five to ten atmospheric samples at one-minute intervals, then sets of 50-100 seawater

92 samples at one-to-two-minute intervals (Pierrot et al. 2009). The standards and atmospheric
93 samples caused small gaps in all the data collected. The sea surface and atmospheric CO₂ (ppm)

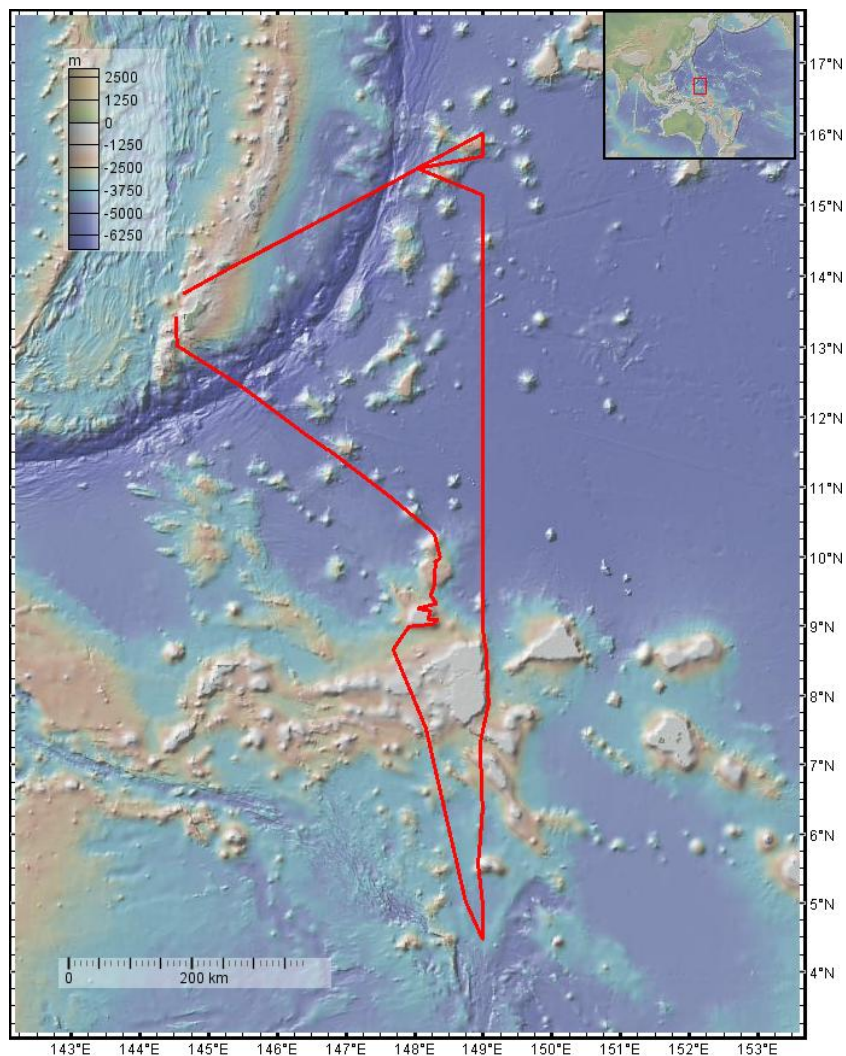


Figure 2. Map of cruise transect from December 29, 2024, to January 9, 2025. Made using GeoMapApp.

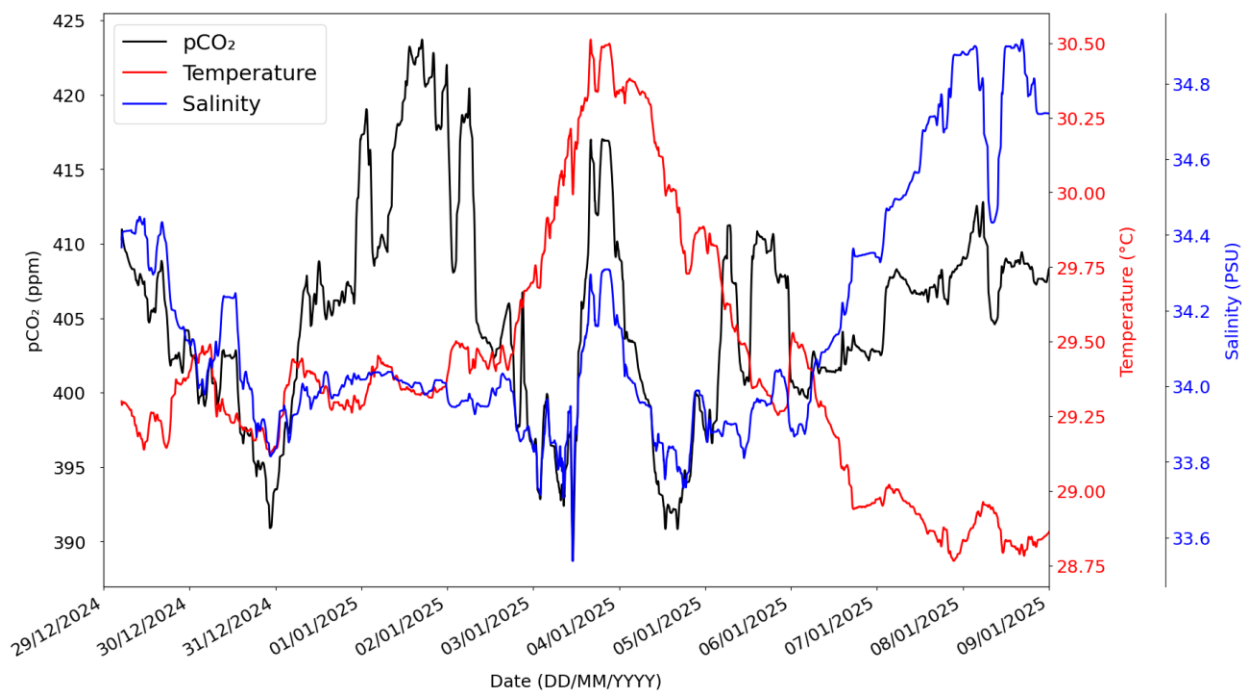
94 levels and oxygen were measured. The same control software contains GPS information from the
95 navigation system, and data from the meteorological sensors of the ship.

96 Measurements from the entire cruise track were analyzed to identify the peaks and
97 troughs in pCO₂ concentrations and identify a correlation among pCO₂ variations, temperature,

98 and salinity. Atmospheric pCO₂ was averaged across the cruise dates since CO₂ has a long
99 lifetime and becomes well-mixed in the atmosphere (Hakkarainen et al. 2016). The average of
100 424.7 ppm was used for ΔpCO₂ calculations.

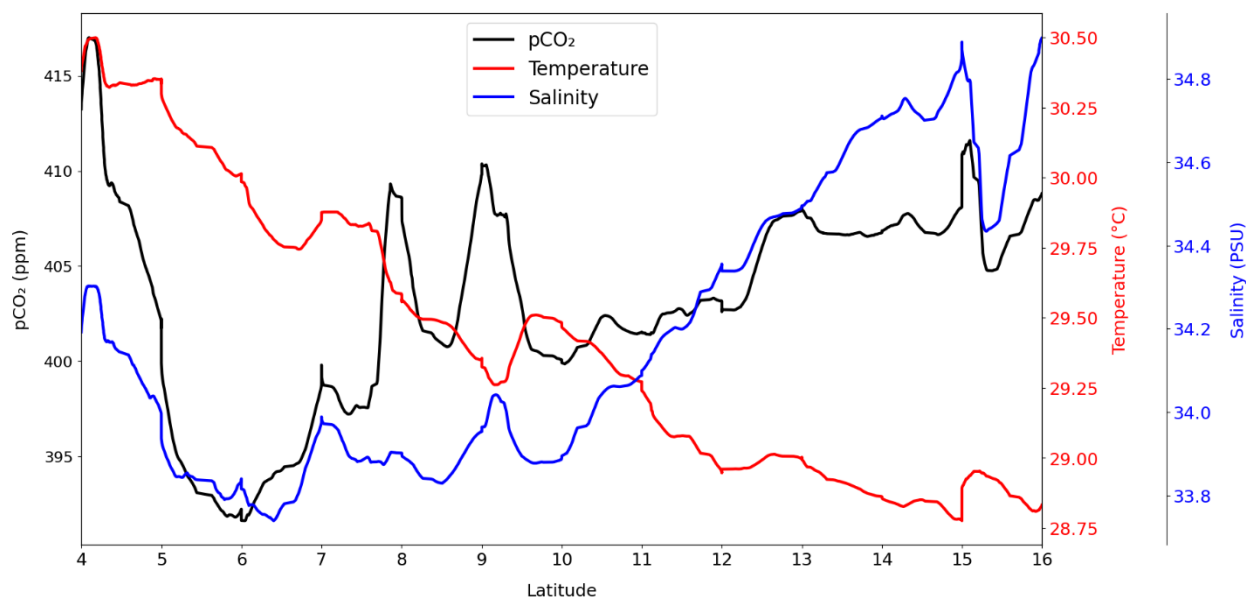
101 3. Results

102 Throughout the two weeks, the highest pCO₂ concentrations up to 424.5 ppm was
103 measured on 1 January 2025, adjacent to Nam-2 Atoll, while the lowest pCO₂ concentrations of
104 391 ppm along with the highest temperatures of 30.5 °C was measured on 3 January 2025 near 5
105 °N along the 149 °E (Fig. 3). The pCO₂ concentration, temperature and salinity all increased on 3
106 January 2025, after this low in pCO₂ (Fig. 3). From 3 January 2025 through 5 January 2025, the
107 greatest range of pCO₂ concentrations were measured at 391-418 ppm. 6 January 2025 through 9
108 January 2025 had the smallest variability with a range of 413-403 ppm. Other low pCO₂
109 concentrations were measured around 5.8 °N-6.1 °N of 392 and another at 9.8 °N of 392 ppm.



110
111 **Figure 3.** Values of pCO₂ in ppm, temperature in °C, and salinity in PSU throughout the cruise
112 dates (DD/MM/YYYY).

113 Overall, temperature had little correlation to pCO₂. The temperature only varied by 1.75
114 °C throughout the whole cruise. On 4 January 2025, there was a pCO₂ concentration of 416 ppm
115 but a temperature of about 30.5 °C. Salinity followed a similar pattern of peaks and troughs as
116 the pCO₂ concentrations, ranging from 33.25-35 PSU. However, on 1 January 2025, salinity
117 stayed steadily around 33.9 PSU despite the largest pCO₂ increase at the Nam-2 Atoll (Fig. 3).
118 High pCO₂ concentrations up to ~418 ppm was measured on 3 January 2025 and 5 January 2025
119 which were when the ship was the closest to the equator, southwards to 4 °N. Temperature was
120 highest with the 3 January 2025 pCO₂ peak then it decreased slightly after this day (Fig. 3).
121 There is a peak in pCO₂ concentrations at 4 °N before it drops down steeply to 393 ppm. With
122 these latitudinal changes, temperatures show an increase southwards while there is a decrease in
123 salinity with only a small peak at 4 °N (Fig. 4).



124
125 **Figure 4.** Concentrations of pCO₂ across latitude for the entire cruise track.

126 Latitudinally, pCO₂ decreases after concentrations of ~418 ppm at 4.1 °N but then
127 increases starting at 5 °N. A slight increase up to ~408 ppm was measured at 8°N before
128 decreasing sharply until a large peak at the Nam-2 Atoll location at 9°N (Fig. 5). Northwards

129 from 9.8 °N, pCO₂ concentrations increase up to 10 ppm. More decreases in concentration to 392
130 ppm were measured between 5.8 °N-6.1 °N (Fig. 3).

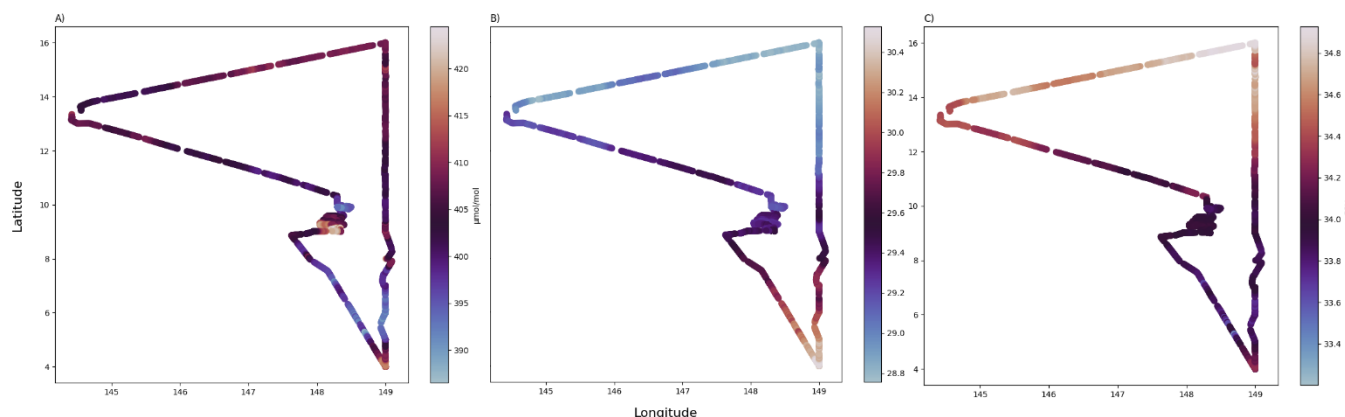
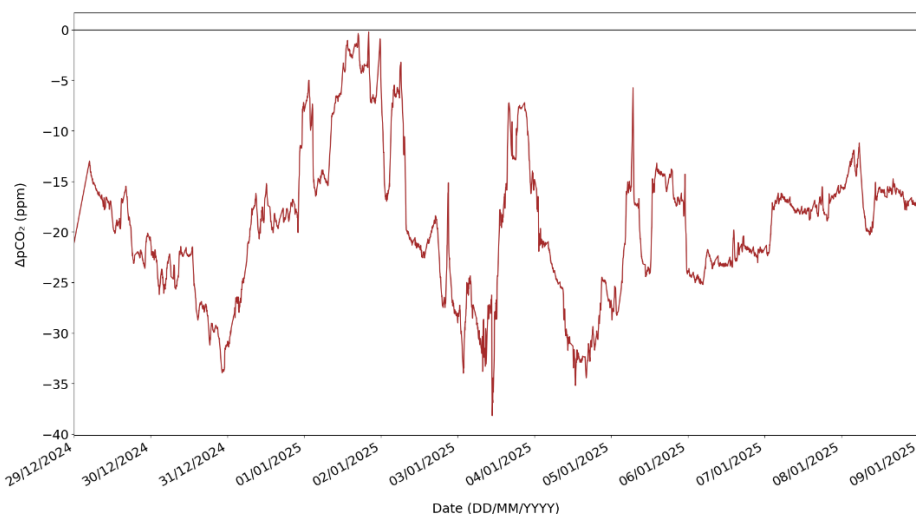


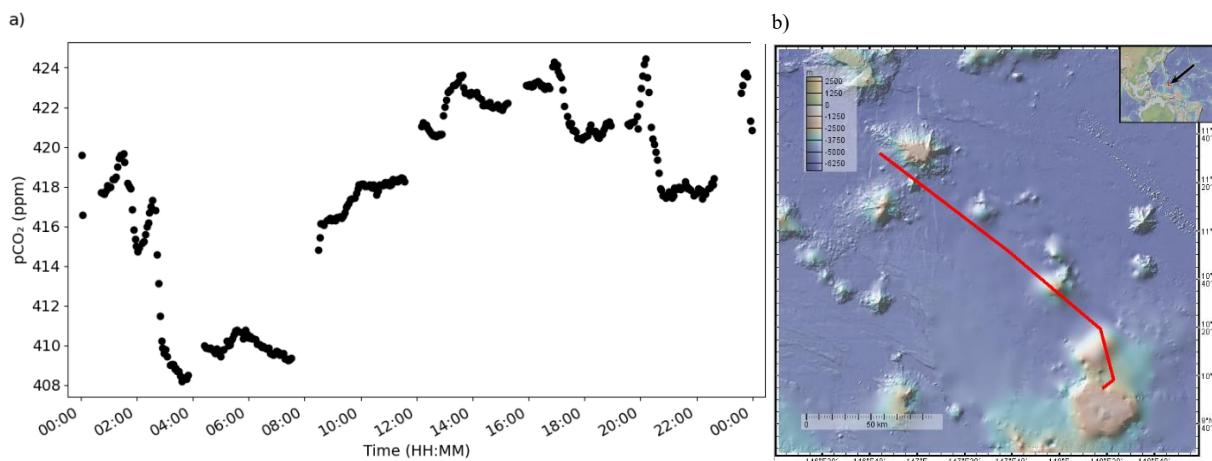
Figure 5. Measurements of a) pCO₂ in ppm, b) temperature in °C, and c) salinity in PSU throughout the cruise across longitude vs. latitude.

131 Based on an average atmospheric pCO₂ concentration of 424.68 ppm, this region remains
132 undersaturated in pCO₂ concentrations up to -38 ppm (Fig. 6). The atoll area does go up to over
133 424 ppm and can be a source of outgassing throughout a longer-time frame.



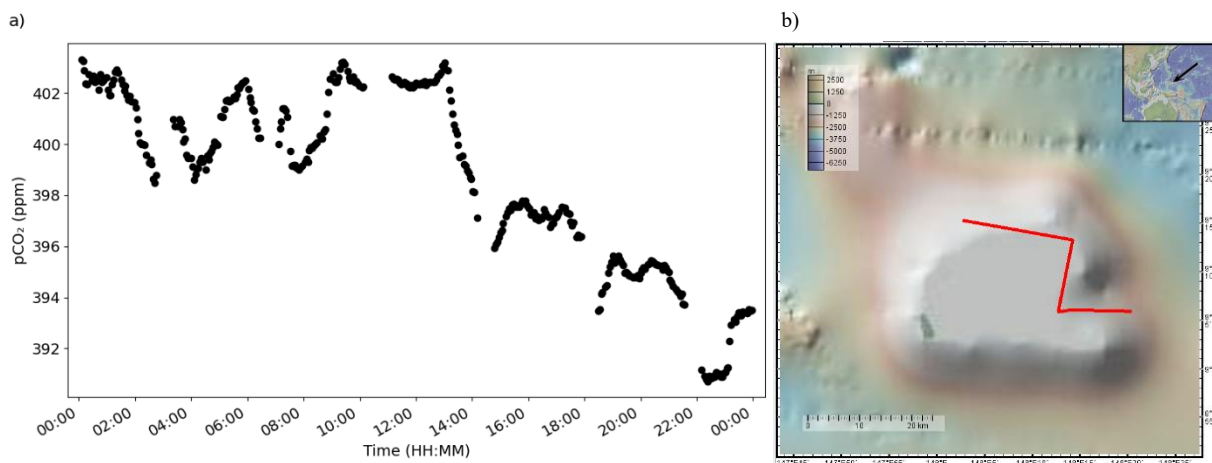
134
135 **Figure 6.** Measurements of ΔpCO₂ for the duration of the cruise. Difference in sea surface pCO₂
136 and averaged (across the cruise dates) atmospheric pCO₂ to get ΔpCO₂. Line at 0 indicates where
137 the ocean would become a source of pCO₂.

138 Around Namonuito Guyot, pCO₂ concentrations range from 392-402 ppm. There is a
139 steep drop in concentrations starting at 1300 on 30/12/2024 when the R/V *Thompson* nears the
140 guyot (Fig. 7).



141
142 **Figure 7.** a) Concentrations of pCO₂ throughout 30 December 2024 from 11.5 °N, 147 °E to 9.91
143 °N, 148 °E approaching Namonuito Guyot (depth of 1500 m). Gaps in data are from the
144 underway pCO₂ system taking standards and atmospheric samples. b) Map of 30/12/2024
145 transect. Made using GeoMapApp.

146 For the atoll location, pCO₂ concentrations range from 410-424 ppm with a steep increase
147 measured at 0830 and concentrations remain around 424 ppm for the rest of this day (Fig. 8).



148
11

149 **Figure 8.** a) Concentrations of pCO₂ throughout 1 January 2025 from 9.26 °N, 148 °E to 9.10°N,
150 148 °E, at Nam-2 Atoll. Gaps in data are from the underway pCO₂ system taking standards and
151 atmospheric samples. Bb) Map of the cruise track on 1 January 2025 over Nam-2 Atoll. Made using
152 GeoMapApp.

153 **4. Discussion**

154 **4.1. Temperature and salinity correlations with pCO₂ vary**

155 The surface seawater pCO₂ ranged from 390-420 ppm, only about 10-20 ppm difference in
156 concentration levels compared to Yasunaka et al. (2019) findings. This cruise only went to 4 °N
157 but there is a signal of increased pCO₂ concentrations from equatorial upwelling. Temperature
158 was lower while salinity was measured to be higher at 4 °N (Fig. 3).

159 The weak correlation between pCO₂ and temperature is due to the region being an area
160 where temperatures hardly fluctuate. The monthly average of Apra Harbor, Guam, the ship's
161 port, spans from 26.4 °C-29.7 °C (NCEI 1994-2022). For this study's cruise, the temperature
162 ranged from 28.8 °C-30.4 °C. This is an increase from 1981-2015 long-term means that gave
163 SST of about 25 °C-28 °C, though the increase is only from two weeks, even with 1 °C of SST
164 anomaly in the region. Based on these ranges, it is expected that pCO₂ would be low (Yasunaka
165 et al. 2019). It is difficult to conclude this due to the limitations of data collection.

166 **4.2. Concentrations of pCO₂ increase with increasing latitude along 149 °E**

167 At 4 °N, 149 °E, pCO₂ concentrations hit a maximum in concentration. This peak was
168 caused by these waters originating from the equatorial upwelling of deeper carbon-rich waters
169 mixed into the surface water (Yasunaka et al. 2019). Upwelling was indicated by slightly higher
170 salinity measured at 34.3 PSU with the temperature measured at 30.5 °C and an increase in NO₃
171 and PO₄ (Fig.4; Claire Sheppard, Personal Communication).

172 After this peak in pCO₂ concentrations, temperatures began decreasing down to 28.8 °C
173 for the rest of the northward transect along 149 °E. Salinity was increasing with this decrease and
174 was measured up to 34.9 PSU (Fig. 4). There were two small increases in salinity aligned with
175 the maxima in pCO₂ concentrations at about 8 °N and 9 °N due to the depth becoming shallow at
176 these areas. There was a steep decline in salinity and pCO₂ concentrations and a 0.75 °C increase
177 at 15 °N where the lowest biological productivity was found (Parthasarathy, Personal
178 Communication).

179 The general trend along 149 °E showed pCO₂ increasing along increasing latitudes. This
180 is the opposite of what was expected, where Yasunaka et al. (2019) found the long-term mean of
181 pCO₂ increasing at the equator to about 5 °N, though if measurements continued closer to the
182 equator, they could have shown the increase continuing from the 4 °N peak due to the equatorial
183 upwelling of CO₂.

184 **4.3. Study region is a sink**

185 All the ΔpCO₂ calculations resulted in negative values. Therefore, this study region was
186 determined to be a sink for CO₂. The pCO₂ over the atoll reaches 424.5 ppm and the atmospheric
187 pCO₂ was at an average of 424.7 ppm for the time of the cruise (Fig. 6). Though a small
188 difference, this is where it becomes crucial to conduct long-term regional-scale studies to
189 identify sources. The atmosphere and ocean will continue to reach equilibrium as pCO₂
190 concentrations change.

191 **4.4. Increase at Nam-2 Atoll vs. decrease at Namonuito Guyot in pCO₂ Concentrations**

192 Seamounts with shallower depths, specifically tested at the Caroline Seamount in the
193 tropical western Pacific, bring on a higher abundance of virioplankton, a marine virus that
194 accounts for a high proportion of bacterial mortality which leads to decay that releases carbon.

195 The combination of a shallow seamount and local currents can support the bacteria's production
196 and abundance (Zhao et al. 2020). The highest pCO₂ concentrations of 424 ppm were also at the
197 deepest section of the Nam-2 Atoll (9.25 °N with a depth of 1000 m) and the steep decrease to
198 393 ppm on 1 January 2025 was seen at the shallowest section where the depth was around 100
199 m at 9.8 °N (Fig. 3). Nam-2 Atoll was found to have the highest biological productivity but the
200 decrease in pCO₂ concentrations disproves the hypothesis (Sheppard & Parthasarathy, Personal
201 Communication).

202 However, with the guyot which has a depth of 1500 m, pCO₂ concentrations steadily
203 decreasing throughout the day closer to the guyot (Fig. 7). This would be due to the weaker
204 vertical mixing in this subtropical region causing the vertical mixing to not reach the surface as
205 it did at the atoll location (Guo et al. 2024). Since Nam-2 Atoll is closer to the surface, higher
206 pCO₂ concentrations come from the mixing while the shallowest section is photosynthesizing
207 and therefore decreasing the concentrations. Namonuito Guyot is deeper and so the local,
208 vertical mixing is not reaching the surface where the pCO₂ measurements were being taken.
209 Additionally, there were no increases in both salinity and temperature, indicating no upwelling
210 of colder, saltier subsurface waters at either location.

211 **5. Conclusion**

212 The key is the shift from sink to source. Seamounts' influences on pCO₂ are localized and
213 small but cause variations from seamount to seamount. The depth of the seamount can be part of
214 whether the area is a source or a sink, and their biological inhabitants are essential to the
215 biogeochemical cycle. Their health is dependent on the ocean's health and vice versa. As marine
216 heatwaves increase in intensity and frequency, subtropical regions such as the one tested in this

217 study need to be measured to ensure conditions do not go beyond irreparable, destroying the
218 habitats and their inhabitants.

219 Spatially, concentrations of pCO₂ can vary enough to make one area a sink and another
220 area a source of CO₂. The local variability leads to difficulty in predictions of CO₂ uptake and
221 further widens the gaps in understanding the biogeochemical cycle. As politics divide around the
222 world about climate change, it becomes even more crucial to accurately inform to place solutions
223 and preventative measurements. This data collection improves the ability to build upon current
224 understanding and further modeling for future predictions.

225 The short duration of the cruise limited data collection and therefore, the analysis of the
226 effects of SST on pCO₂ concentrations. Further long-term study of regional analyses where
227 specific factors, such as bathymetry, wind speeds, and oxygen, are needed to connect the regional
228 spatial-temporal variations because specific regions will react differently based on these factors.
229 Regional-scale analysis, specifically increased sampling of varying seamounts features and the
230 variability of pCO₂ concentrations across them must be emphasized for regional sea-air flux
231 measurements and understanding, especially as anthropogenic CO₂ emissions and temperatures
232 continue rising.

233 **Acknowledgments**

234 The author thanks the Research Vessel *Thomas G. Thompson* captain and crew for their
235 support throughout the TN 440 cruise. Support and access to preliminary data for the underway
236 pCO₂ system from NOAA PMEL and Dr. Simone Alin, PI, is also acknowledged. The author is
237 grateful to the School of Oceanography and the Korean Student Association Careers winter
238 research grant at the University of Washington for their financial support to make this project

239 possible. Special thank you to the professors and peers of the Ocean 443-445 series, especially
240 Professor Mark Warner for his mentorship throughout the project.

241 **References**

- 242 Feely, R. A., Takahashi, T., Wanninkhof, R., McPhaden, M. J., Cosca, C. E., Sutherland, S. C.,
243 & Carr, M. (2006). Decadal variability of the air-sea CO₂ fluxes in the equatorial Pacific
244 Ocean. *Journal of Geophysical Research: Oceans*, *111*(C8), 2005JC003129.
245 <https://doi.org/10.1029/2005JC003129>
- 246 Friedlingstein, P., O’Sullivan, M., Jones, M. W., Andrew, R. M., Gregor, L., Hauck, J., Le
247 Quéré, C., Lujikx, I. T., Olsen, A., Peters, G. P., Peters, W., Pongratz, J., Schwingshackl,
248 C., Sitch, S., Canadell, J. G., Ciais, P., Jackson, R. B., Alin, S. R., Alkama, R., ... Zheng,
249 B. (2022). Global carbon budget 2022. *Earth System Science Data*, *14*(11), 4811–4900.
250 <https://doi.org/10.5194/essd-14-4811-2022>
- 251 Guo, Y., & Timmermans, M. (2024). Global ocean *p* CO₂ variation regimes: Spatial patterns and
252 the emergence of a hybrid regime. *Journal of Geophysical Research: Oceans*, *129*(5),
253 e2023JC020679. <https://doi.org/10.1029/2023JC020679>
- 254 Hakkarainen, J., Ialongo, I., & Tamminen, J. (2016). Direct space-based observations of
255 anthropogenic CO₂ emission areas from OCO-2. *Geophysical Research Letters*, *43*(21).
256 <https://doi.org/10.1002/2016GL070885>
- 257 *Home: NOAA physical sciences laboratory*. (n.d.). Retrieved February 21, 2025, from
258 <https://psl.noaa.gov/>
- 259 Jacox, M. G., Alexander, M. A., Amaya, D., Becker, E., Bograd, S. J., Brodie, S., Hazen, E. L.,
260 Pozo Buil, M., & Tommasi, D. (2022). Global seasonal forecasts of marine heatwaves.
261 *Nature*, *604*(7906), 486–490. <https://doi.org/10.1038/s41586-022-04573-9>
- 262 Jiang, L.-Q., Kozyr, A., Relph, J. M., Ronje, E. I., Kamb, L., Burger, E., Myer, J., Nguyen, L.,
263 Arzayus, K. M., Boyer, T., Cross, S., Garcia, H., Hogan, P., Larsen, K., & Parsons, A. R.

264 (2023). The ocean carbon and acidification data system. *Scientific Data*, 10, 136.
265 <https://doi.org/10.1038/s41597-023-02042-0>

266 Lan, X., Tans, P., Thoning, K., & NOAA Global Monitoring Laboratory. (2023). *Trends in*
267 *globally-averaged CO₂ determined from NOAA Global Monitoring Laboratory*
268 *measurements*. [Dataset]. NOAA GML. <https://doi.org/10.15138/9N0H-ZH07>

269 Li, C., Burger, F. A., Raible, C. C., & Frölicher, T. L. (2024). Observed regional impacts of
270 marine heatwaves on sea-air CO₂ exchange. *Geophysical Research Letters*, 51(24),
271 e2024GL110379. <https://doi.org/10.1029/2024GL110379>

272 *Ncei coastal water temperature guide—All coastal regions table*. (n.d.). Retrieved February 21,
273 2025, from [https://www.ncei.noaa.gov/access/coastal-water-temperature-](https://www.ncei.noaa.gov/access/coastal-water-temperature-guide/all_table.html#spac)
274 [guide/all_table.html#spac](https://www.ncei.noaa.gov/access/coastal-water-temperature-guide/all_table.html#spac)

275 Pierrot, D., Neill, C., Sullivan, K., Castle, R., Wanninkhof, R., Lüger, H., Johannessen, T.,
276 Olsen, A., Feely, R. A., & Cosca, C. E. (2009). Recommendations for autonomous
277 underway pCO₂ measuring systems and data-reduction routines. *Deep Sea Research Part*
278 *II: Topical Studies in Oceanography*, 56(8–10), 512–522.
279 <https://doi.org/10.1016/j.dsr2.2008.12.005>

280 Takahashi, T., Feely, R. A., Weiss, R. F., Wanninkhof, R. H., Chipman, D. W., Sutherland, S.
281 C., & Takahashi, T. T. (1997). Global air-sea flux of CO₂: An estimate based on
282 measurements of sea–air pCO₂ difference. *Proceedings of the National Academy of*
283 *Sciences*, 94(16), 8292–8299. <https://doi.org/10.1073/pnas.94.16.8292>

284 Yan, H., Yu, K., Shi, Q., Lin, Z., Zhao, M., Tao, S., Liu, G., & Zhang, H. (2018). Air-sea CO₂
285 fluxes and spatial distribution of seawater pCO₂ in Yongle Atoll, northern-central South

286 China Sea. *Continental Shelf Research*, 165, 71–77.
287 <https://doi.org/10.1016/j.csr.2018.06.008>

288 Yasunaka, S., Kouketsu, S., Strutton, P. G., Sutton, A. J., Murata, A., Nakaoka, S., & Nojiri, Y.
289 (2019). Spatio-temporal variability of surface water $p\text{CO}_2$ and nutrients in the tropical
290 Pacific from 1981 to 2015. *Deep Sea Research Part II: Topical Studies in Oceanography*,
291 169–170, 104680. <https://doi.org/10.1016/j.dsr2.2019.104680>

292 Zhao, Y., Zhao, Y., Zheng, S., Zhao, L., Li, X., Zhang, W., Grégori, G., & Xiao, T. (2020).
293 Virioplankton distribution in the tropical western Pacific Ocean in the vicinity of a
294 seamount. *MicrobiologyOpen*, 9(6), 1207–1224. <https://doi.org/10.1002/mbo3.1031>